Геология и геофизика, *т. 65, № 4, с. 613—628*, DOI: 10.15372/GiG2023166, EDN: FFMQSU
Поступила в редакцию 14.02.2023, принята в печать 29.08.2023 *Опубликована онлайн: 31.08.2024*

УДК 550.4+552.52(514)

ГЕОХИМИЧЕСКАЯ ХАРАКТЕРИСТИКА И ГЕОЛОГИЧЕСКОЕ ЗНАЧЕНИЕ ГЛИНИСТЫХ СЛАНЦЕВ ВТОРОЙ ПАЧКИ ПЕРМСКОЙ СВИТЫ ЛУКАОГОУ В ДЖИМСАРСКОМ ПРОГИБЕ ДЖУНГАРСКОГО БАССЕЙНА (*Северо-Западный Китай*)

Ц. Цзинь[1], Ц. Лю[1], Ч. Лу[2], Ц. Ван[1], Ц. Ли[2], Ж. Чжу[2], Ю. Ван[2]

[1]*Research Institute of Experiment and Detection, Petro China Xinjiang Oilfield Company, Xinjiang, 834000, China*

[2]*Institute of Ocean College, Zhejiang University, Zhejiang, 316000, China*

Формация Лукаогоу в Джимсарском прогибе является важным продуктивным пластом сланцевой нефти в Джунгарском бассейне. В данной работе информация о керне, содержании органического углерода и углеводородных биомаркерах, а также результаты пиролиза горных пород и разделения компонентов органического вещества были использованы для изучения обстановки осадконакопления, типа исходного материала, зрелости органического вещества и нефтеносных свойств глинистых сланцев второй пачки формации Лукаогоу. Полученные результаты показали полуокислительную-полувосстановительную обстановку осадконакопления. Исходный материал был в основном аквагенным с незначительной примесью высших растений. Среднее общее содержание органического углерода (TOC) составляет 7.43 %, среднее значение генерационного потенциала углеводородов (S_1 + S_2) — 50.54 мг/г, а средняя температура T_{max} составляет 446 ºС, что указывает на высокую зрелость глинистого сланца. Хлороформный битум «А» отличается высоким содержанием предельных углеводородов (в среднем 34.10 %), низким содержанием ароматических углеводородов (в среднем 15.39 %) и высоким соотношением насыщенных и ароматических углеводородов (2.54). По числу атомов углерода насыщенные углеводороды находятся в интервале между *n*-C_{13} и *n*-C_{33}. Спектры их распределения демонстрируют преобладание алканов средней и низкой молекулярной массы, основные пики приходятся на *n*-C_{17} и *n*-C_{23}. Среднее значение $\Sigma C_{21}^{-}/\Sigma C_{22}^{+}$ составляет 1.19, что указывает на преобладание алканов с короткой цепью. Глинистые сланцы второй пачки формации Лукаогоу характеризуются большой мощностью, высоким содержанием органического вещества и высоким нефтегенерационным потенциалом. Они являются перспективным объектом для добычи сланцевой нефти в Джимсарском прогибе и имеют важное значение для поисково-разведочных работ в будущем.

Джунгарский бассейн, формация Лукаогоуб, глинистый сланец, геохимические характеристики, геологическое значение

GEOCHEMICAL CHARACTERISTICS AND GEOLOGICAL SIGNIFICANCE OF MUD SHALE OF THE SECOND MEMBER, PERMIAN LUCAOGOU FORMATION, JIMSAR SAG (*Junggar Basin, NW China*)

J. Jin, J. Liu, Z. Lou, J. Wang, J. Li, R. Zhu, Y. Wang

The Lucaogou Formation in Jimsar sag is an important shale oil-producing layer in the Junggar basin. In this paper, core data, organic carbon, rock pyrolysis, biomarker compounds, and organic matter group component separation were used to study the sedimentary environment, parent material type, organic maturity and oil-bearing property of mud shale of the Second member of the Lucaogou Formation. The results showed that the sedimentary environment is a semi-oxidation and semi-reduction environment. The parent material is mainly aquatic with minor input of higher plants. The average TOC is 7.43%, the average value of hydrocarbon generation potential (S_1+S_2) is 50.54 mg/g, and the average value of T_{max} is 446 °C, showing high maturity of the mud shale. The chloroform bitumen “A” features high saturated hydrocarbon content (34.10% on average), low aromatic hydrocarbon content (15.39% on average), and high saturated/aromatic ratio (2.54). The carbon number of saturated hydrocarbons is distributed between *n*-C_{13} and *n*-C_{33}. Their peak are mainly *n*-C_{17} and *n*-C_{23}, which are biased toward medium-low molecular weight alkanes. The average of the $\Sigma C_{21}^{-}/\Sigma C_{22}^{+}$ is 1.19, indicating that the alkane has advantage of short chain. The mud shale in the Second member of the Lucaogou Formation has a large sedimentary thickness, high organic matter content, and high oil generation potential. It is an important replacement target for shale oil in Jimsar sag and has important exploration significance in the future.

Junggar basin, Lucaogou Formation, mud shale, geochemical characteristics, geological significance

© Цзинь Ц., Лю Ц., Лу Ч., Ван Ц., Ли Ц.✉, Чжу Ж., Ван Ю., 2024

✉e-mail: 12034074@zju.edu.cn

INTRODUCTION

Shale oil refers to the oil that occurs in black organic-rich shale (Zou et al., 2013), or relatively high porosity and permeability reservoirs in shale systems, such as tight sandstone and tight carbonate rock (Hu et al., 2020). With the continuous progress of exploration and development technology, shale oil has gradually become an important field for oil exploration in the 21st century (Tong et al., 2018; Hu et al., 2020). According to the paleo-sedimentary environment, shale oil is mainly divided into two types: continental facies and marine facies (Zou et al., 2013; Wang et al., 2022a, b). At present, the major shale oil-producing areas in the world are mainly marine facies. The Bakken Formation in the Williston basin (Eidsnes, 2014), the Bazhenov Formation in the West Siberian basin (Zanin et al., 2008; Skvortsov et al., 2017), and the Eagle Ford in Gulf Goast basin (Hou et al., 2021) are typical representatives. Shale oil in China mainly belongs to continental shale oil, which is typically represented by the Yanchang Formation in the Ordos basin, the Shahejie Formation in the Bohai Bay basin, and the Lucaogou Formation in the Junggar basin (Yang et al., 2016, 2019; Du et al., 2019). Compared with marine shale oil systems, continental shale oil reservoirs have higher heterogeneity, showing the characteristics of frequent mud-sand interbeds and multi-scale cycles. Different cycles have huge differences in source rock properties, sand body lithology, physical properties, and pore structure (Qiu et al., 2016; Pang et al., 2017; Li et al., 2022; Hu et al., 2022). The common problems in Chinese continental shale oil are: 1) the relationship between the frequently interbedded mud shale and tight sand layer in generation, transportation and storage of the shale oil; 2) the hydrocarbon generation potential of the mud shale; 3) the influence of the paleo-sedimentary environment on the migration and accumulation of hydrocarbons. These problems limit the large-scale and profitable development of continental shale oil in China. The sedimentary environment of continental shale oil is changeable, the quality of mud shale is uneven, and the reservoir often shows strong heterogeneity (Zhao et al., 2020; Wang et al., 2020; Hu et al., 2022). So, as the dual carrier of hydrocarbon generation and reservoir formation, the sedimentary environment and organic geochemical characteristics of mud shale are the focus of continental shale oil research.

The Jimsar sag in the southeastern margin of the Junggar basin is currently the largest experimental area for shale oil development in China. The shale oil-producing layers are mainly the Middle Permian Lucaogou Formation, which has shale oil reserves of 1.112 billion tons, and it's crude oil production is expected to reach 2 mln tons by 2025. It plays an important role in ensuring national energy security and promoting local economic development and social stability. The shale oil of the Lucaogou Formation in Jimsar sag belongs to continental shale oil with complicated sedimentary and burial history. Which results the complex mixed rocks, including terrigenous clastic components, pyroclastic components and carbonate components. The lithology changes rapidly and frequently interbed (Qiu et al., 2016). There is no clear boundary between the source rock and reservoir rock, and the oil layer is thin and uneven (Bai et al., 2017; Wang et al., 2020), which is different from the marine shale oil in North America (Eidsnes, 2014; Li et al., 2019). In previous studies, the Lucaogou Formation was often studied as tight oil. It was believed that only tight carbonates and fine-grained clastic rocks had storage capacity and development potential (Wu et al., 2016; Cao et al., 2017). With a deeper understanding, it was realized that the complex mud-sand interbed system makes the Lucaogou Formation possess the characteristics of shale oil at the same time, which cannot be simply studied as tight oil (Gao et al., 2020). However, there are still some gaps in the understanding of such system, including 1) what kind of paleo-sedimentary environment did frequent sand-mud interbeds form in, 2) whether the mud shale has hydrocarbon generation potential, and 3) whether it is suitable for exploitation in multilayer mud shale strata. The study of these problems will help to understand the genesis and enrichment pattern of shale oil in Lucaogou Formation of the Jimsar sag.

In this paper, the Second member of the Lucaogou Formation was taken as the research object, and the experiments and analysis of organic carbon, rock pyrolysis, biomarker compounds, and organic matter group components were carried out. Although previous studies have extensively investigated the stratigraphy and hydrocarbon source rock characteristics of the Lucaogou Formation based on the exploration results from well Ji 174, there has been no mention of the depositional paleoenvironment of the Lucaogou Formation. Moreover, with subsequent exploration, it was discovered that well Ji 174 is not located in the most favorable area for oil and gas generation. Therefore, the preliminary understanding based on well Ji 174 is not accurate. Through the study of the key exploration well, J10025, at present, the sedimentary environment, parent material type, maturity, oil-bearing property and shale oil geological significance of mud shale in the Second member of the Lucaogou Formation were studied. The purpose is to provide geological theoretical guidance for the next step of exploration and development of shale oil in the Second member of the Lucaogou Formation in Jimsar sag.

GEOLOGICAL OVERVIEW

The Jimsar sag is located southwest of the eastern uplift of the Junggar basin (Fig. 1*a*). It is a dustpan-shaped sag developed on the early Carboniferous folded basement (Xiao et al., 2008). The interior topography of the sag is gentle and the structure is single. The periphery is bounded by faults, including the Jimsar fault in

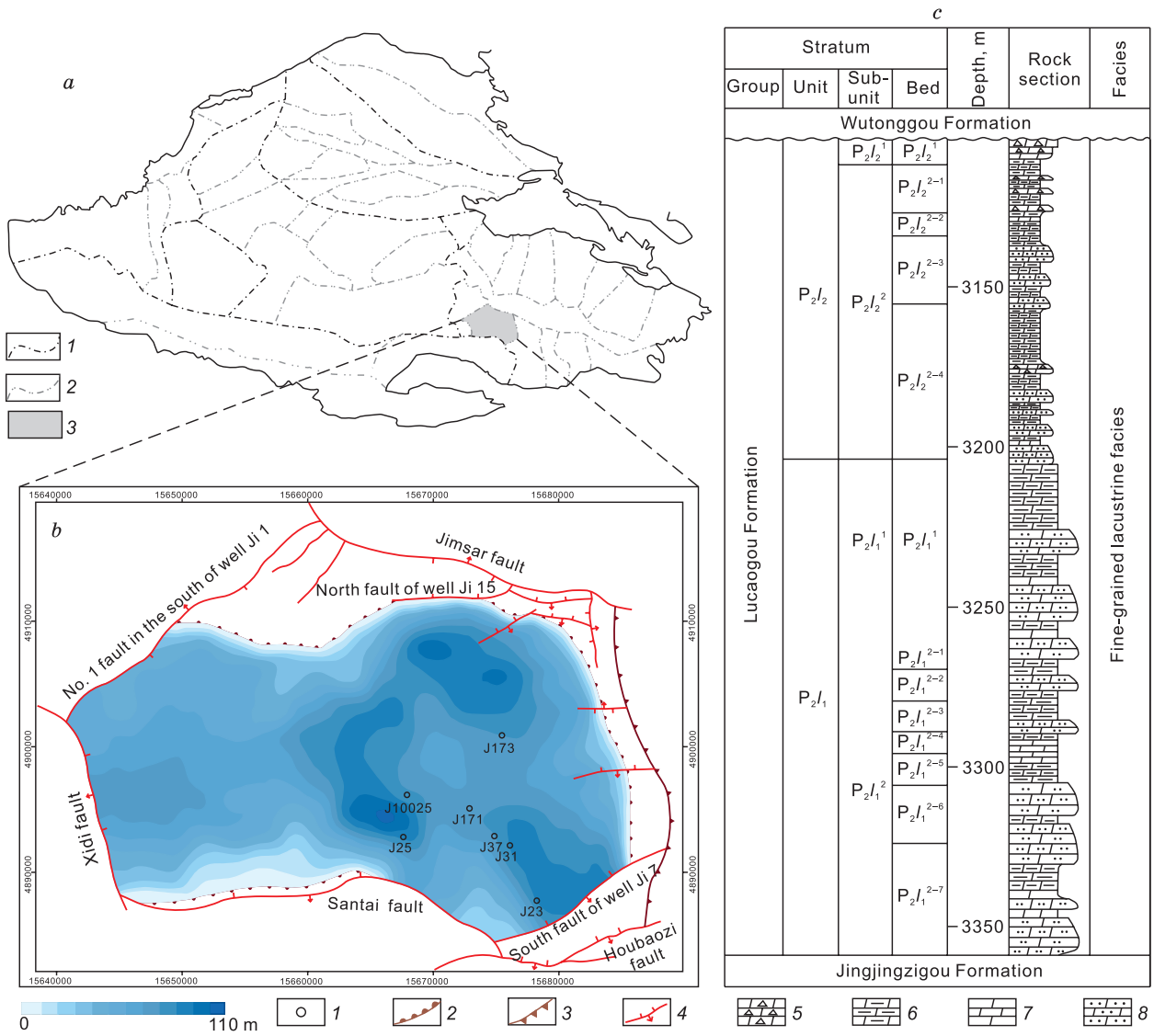

Fig. 1. Geological overview of the Lucaogou Formation in Jimsar sag.

a – the location of the sag in the basin: *1* – primary tectonic line, *2* – secondary tectonic line, *3* – Jimgar sag; *b* – distribution of tectonics and hydrocarbon source rocks; *c* – the overall stratigraphic characteristics: *1* – industrial oil wells, *2* – source rock boundary, *3* – stratigraphic boundary, *4* – fault, *5* – sand-clasic dolomite, *6* – dolomitic mudstone, *7* – microcrystalline dolomite, *8* – dolomitic silstone.

the north, the Santai fault in the south, the No.1 fault in the south of Ji 1 and the Xidi fault in the west. It gradually uplifted to the east, transitioning to the Qitai bulge. The sag generally shows a monoclinic shape of "high in the east and low in the west", covering an area of 1278 km^2 (Kong et al., 2021) (Fig. 1*b*). Jimsar sag has experienced four periods of tectonic activity: Hercynian, Indosinian, Yanshanian, and Himalayan. The Lucaogou Formation was deposited during the Middle Jurassic period, and is not only an important source rock but also an essential reservoir. The strong tectonic movement in the northern Tianshan Mountains in the Permian period led to structural subsidence, which provided accommodating space for sediments (Fang et al., 2006). After a long geological process, the Lucaogou Formation formed the present shale system. The typical feature of this shale system is that the source rocks and reservoir are frequently interbedded without obvious boundaries. The oil reservoir has strong heterogeneity and is difficult to explore.

Sedimentary facies studies show that the provenance of the Permian Lucaogou Formation in the Jimsar sag mainly comes from the surrounding paleo-uplifts. The Lucaogou Formation is a set of fine-grained lacustrine sedimentary system, including deep lacustrine and shallow lacustrine. The Lucaogou Formation is unconformably overlain by the Wutonggou Formation, and in a conformable contact with the underlying Jingzigou Formation. It can be divided into two segments, namely the Lower Lucaogou Formation (P_2l_1) and the Upper

Lucaogou Formation (P_2l_2), from bottom to top. Each section can be further divided into several sublayers (Fig. 1*c*). And the sedimentary history is a lake transgression process (Qu et al., 2019). The burial depth is the largest in the southwestern part of the sag near the Xidi fault, and it is gradually uplifted and denuded in the east, northeast and northwest directions (Qiu et al., 2016). The distribution of the source rocks in the Second member of the Lucaogou Formation is shown in Fig. 1*b*. The thickness distribution of the source rock is relatively stable, the thickest is 110 m, which is located near J10025 well in the middle of the Jimsar sag (Fig. 1*b*).

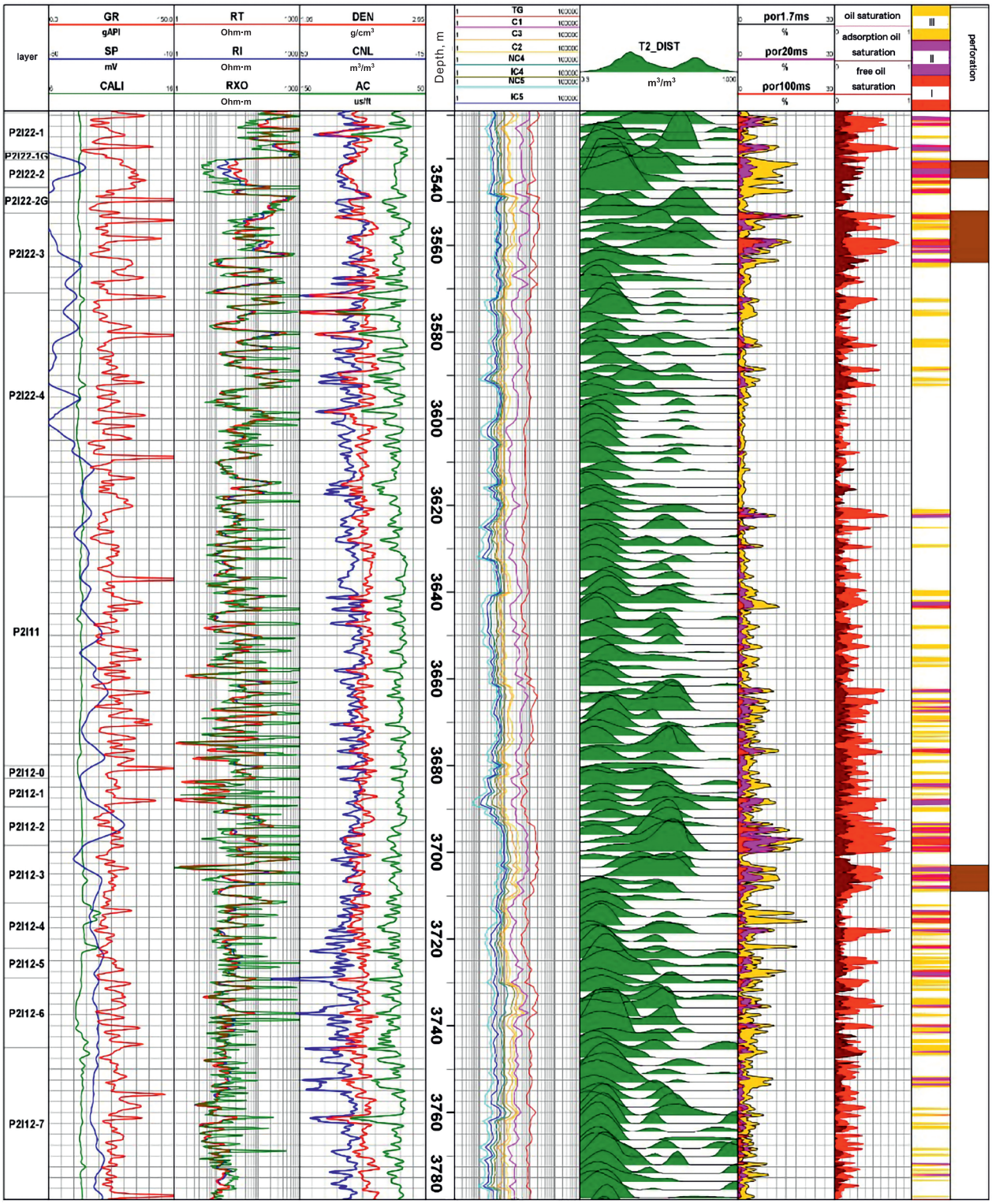

Fig. 2. Comprehensive logging interpretation of J10025.

The structural location of well J10025 belongs to the southeastern slope area of the Jimsar sag. Comprehensive logging interpretation shows that the depth of the Lucaogou Formation is 3530–3780 m and it is divided into upper and lower layers. Among them, the Second member of the Lucaogou Formation has a buried depth of 3530–3618 m, and is divided into two sublayers: $P_2l_2^1$ and $P_2l_2^2$. The lithology of $P_2l_2^1$ is mainly gray mud shale. It is not only the source rock, but also the cap of the lower reservoir. The RT ranges from 30.0 to 1000.0 Ohm·m and the DEN distribution ranges from 2.11 to 2.63 g/cm^3 (Fig. 2). It indicates that the porosity and permeability of $P_2l_2^1$ are very low. The lithology of $P_2l_2^2$ is mainly gray sand-clastic dolomite, argillaceous siltstone, dolomite-clastic sandstone mixed with gray mud shale and cloud mud shale. The RT is between 10.0 and 800.0 Ohm·m, the DEN is between 1.96 and 2.57 g/cm^3 (Fig. 2). It is consistent with the complex lithology and good reservoir characteristics of $P_2l_2^2$. From the current development situation, the exploration effect of $P_2l_2^2$ is good. The oil-producing wells in the Second member of the Lucaogou Formation, including Ji 25, Ji 171, Ji 173, Ji 23, Ji 31, and Ji 37, the oil-producing intervals are all $P_2l_2^2$.

SAMPLES AND EXPERIMENTS

We collected 14 mud shale samples of different depths and layers in the Second member of the Lucaogou Formation of J10025. The message of the sample is shown in Table 1. Soxhlet extraction was used for the soluble organic matter in mud shale. First, the samples were crushed and screened by 100 mesh, and then a 200 g powder sample was extracted continuously for 72 hours by Soxhlet extraction. The extraction reagents were chloroform and methanol, the volume ratio of them was 98 : 2, and the extraction temperature was 75 °C. The extracted chloroform bitumen was concentrated to 3–5 mL on a rotary evaporator, volatilized and dried naturally under the temperature did not exceed 40 °C, and was stored in a desiccator for later use. The organic matter group component separation adopts the SY/T 5119-2008 standard. Using the silica gel and alumina chromatographic columns. Benzene, *n*-hexane and absolute ethanol were used as rinsing agents. Through the column chromatography, the saturated hydrocarbons, aromatic hydrocarbons and non-hydrocarbons were obtained. The model of gas chromatograph used in saturated hydrocarbon chromatography experiment was 6890N. And the detection standard was SY/T 5779-2008. The model of chromatograph/mass spectrometer was MS220-0251, and the detection standard was GB/T 18606-2001. Rock pyrolysis was conducted using the ROCK-EVAL 6 pyrolysis instrument with equipment number E90665192, following the detection guidelines outlined in GB/T 18602-2012. All experiments were completed in the experimental center of the Exploration and Development Research Institute of Xinjiang Oilfield Company.

GEOCHEMICAL CHARACTERISTICS

Characteristics of paleo-sedimentary environment

Biomarker compounds are complex molecular fossils that have developed from biochemical substances in previously living organisms. They show a certain degree of stability during the evolution of organic matter,

Table 1. **Sample group component and extracts physical properties parameters**

Sample No.	Depth, m	Layer	Composition	Density, g/cm^{-3}	Viscosity, mPa·s	*w*(saturated hydrocarbons), %	*w*(aromatic hydrocarbons), %	*w*(colloid), %	*w*(asphaltene), %	Saturated/aromatic
1	3535.12	$P_2l_2^1$	Black mud shale	0.87	45.00	23.76	20.30	35.89	13.37	1.17
2	3546.17	$P_2l_2^{2-1}$	Black mud shale	0.87	32.32	15.07	9.04	54.25	16.16	1.67
3	3561.85	$P_2l_2^{2-2}$	Black mud shale	0.87	62.48	43.16	17.43	30.83	6.17	2.48
4	3569.20	$P_2l_2^{2-3}$	Black mud shale	0.87	43.58	21.15	16.01	49.55	7.25	1.32
5	3597.10	$P_2l_2^{2-3}$	Dark grey mud shale	0.88	49.94	52.49	8.05	24.90	4.60	6.52
6	3603.05	$P_2l_2^{2-3}$	Black mud shale	0.88	34.44	32.99	10.07	35.42	12.85	3.28
7	3624.30	$P_2l_2^{2-3}$	Dark grey mud shale	0.89	48.78	49.26	10.00	20.37	13.33	4.93
8	3639.65	$P_2l_2^{2-4}$	Dark grey mud shale	0.89	34.12	16.06	20.88	45.38	11.24	0.77
9	3640.65	$P_2l_2^{2-4}$	Black mud shale	0.89	48.63	36.34	20.19	35.40	9.01	1.80
10	3656.60	$P_2l_2^{2-4}$	Dark grey mud shale	0.88	34.63	40.24	19.12	31.47	11.55	2.10
11	3657.30	$P_2l_2^{2-4}$	Black mud shale	0.89	53.63	51.61	13.23	32.26	1.94	3.90
12	3670.10	$P_2l_2^{2-4}$	Black mud shale	0.89	37.14	28.66	17.20	50.32	7.96	1.67
13	3679.60	$P_2l_2^{2-4}$	Black mud shale	0.90	54.06	21.05	17.29	45.11	19.17	1.22
14	3680.42	$P_2l_2^{2-4}$	Dark grey mud shale	0.90	39.06	45.57	16.67	28.65	7.29	2.73

Table 2. **Biomarker compound parameters**

Sample No.	Depth, m	Layer	A	B	C	D	E	F	G	H	I	J
1	3535.12	$P_2l_2^1$	0.32	0.30	0.12	0.55	0.75	0.58	0.55	0.42	0.37	1.17
2	3546.17	$P_2l_2^1$	0.13	3.72	0.10	0.79	1.23	0.61	0.30	0.45	0.34	1.08
3	3561.85	$P_2l_2^{2-1}$	0.09	0.93	0.18	0.71	1.03	0.59	0.26	0.38	0.30	1.17
4	3569.20	$P_2l_2^{2-1}$	0.10	–	0.11	0.72	1.02	0.59	0.34	0.41	0.32	1.10
5	3597.10	$P_2l_2^{2-2}$	0.10	–	0.19	0.93	1.25	0.57	0.23	0.51	0.40	1.22
6	3603.05	$P_2l_2^{2-2}$	0.26	–	0.14	0.46	0.58	0.56	0.72	0.54	0.29	1.30
7	3624.30	$P_2l_2^{2-2}$	0.09	0.06	0.09	0.51	0.75	0.59	0.40	0.41	0.29	1.12
8	3639.65	$P_2l_2^{2-3}$	0.08	0.50	0.10	0.46	0.73	0.61	0.35	0.38	0.30	0.95
9	3640.65	$P_2l_2^{2-3}$	0.09	0.05	0.10	0.72	1.03	0.59	0.30	0.40	0.30	1.33
10	3656.60	$P_2l_2^{2-4}$	0.10	–	0.25	1.02	1.33	0.57	0.71	0.48	0.30	1.11
11	3657.30	$P_2l_2^{2-4}$	0.04	0.29	0.17	0.59	0.75	0.56	0.55	0.48	0.34	1.06
12	3670.10	$P_2l_2^{2-4}$	0.04	0.33	0.29	1.19	1.47	0.55	0.63	0.45	0.34	0.80
13	3679.60	$P_2l_2^{2-4}$	0.04	0.15	0.30	1.18	1.37	0.54	0.69	0.45	0.34	1.13
14	3680.42	$P_2l_2^{2-4}$	0.06	0.78	0.26	1.05	1.30	0.55	0.13	0.50	0.37	1.08

Note: A – $T_s/(T_s+T_m)$; B – *w*(β-carotene)/*w*(*n*–C_{max}); C – *w*(gammacerane)/*w*(C_{30} hopane); D –*w*(gammacerane)/*w*(C_{31}R hopane); E – *w*(gammacerane)/*w*(C_{31} homohopane); F – 22S/(22S+22R) of C_{31} hopane; G – *w*(C_{27} rearranged sterane 20S)/[*w*(C_{27} rearranged sterane 20(S+R)]; H – C_{29}20S/(20S+20R); I – C_{29}ββ/(ββ+αα); J – *w*(Pr)/*w*(Ph).

essentially preserving the carbon skeleton characteristics of the original biochemical components. Therefore, biomarker compounds, also known as fingerprint fossils, can be utilized to identify the paleo-sedimentary environment (Moldowan et al., 1985; Peters et al., 2005).

Redox property

The ratio of pristane to phytane (Pr/Ph), is a good parameter that can indicate the type of parent material and the depositional environment (Powell and Mckirdy, 1973; Didyk et al., 1978; Ten et al., 1987; Peters et al., 2007). The production of pristane and phytane is related to the photosynthesis of chlorophyll. Chlorophyll produces phytane through photosynthesis under reducing conditions and pristane under oxidative conditions. The high abundance of phytane reflects the strong reducing and high salinity sedimentary environment. The predominance of pristane content reflects the oxidative environment (Didyk et al., 1978). It is generally believed that the *w*(Pr)/*w*(Ph) of source rocks in a oxidative environment is greater than 2. The value in the semi-oxidizing and semi-reducing environment is 1–2. And the value in a reducing environment is less than 1 (Peters et al., 2005). The *w*(Pr)/*w*(Ph) of the samples range from 0.80 to 1.33, with an average value of 1.12 (Table 2). The contents of pristane and phytane are similar, indicating that the paleo-sedimentary environment was a semi-oxidative and semi-reductive environment.

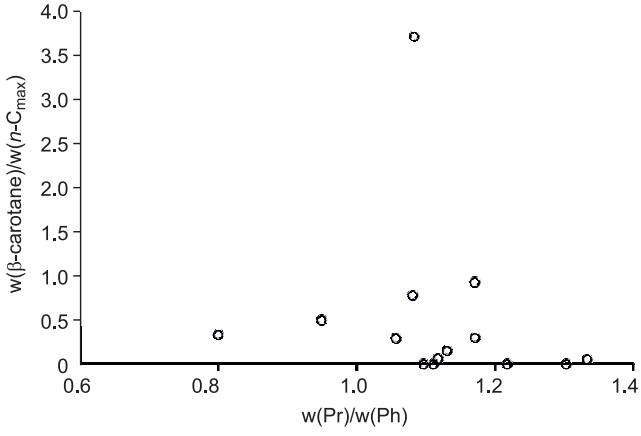

Fig. 3. Crossplot of Pr/Ph and *w*(β-carotane)/*w*(*n*-C_{max}).

The β-carotane is a high-carbon tetraterpenoid saturated hydrocarbon, and its existence is usually mainly attributed to the input of bacteria and algae organic matter in anoxic, saline lake sediments (Schoell et al., 1994). Its precursors appear as pigments in some algae, and are most abundant in halophilic archaea and photosynthetic bacteria, especially photosynthetic bacteria are found in almost all lakes with stratified water bodies (Schoell et al., 1994). Therefore, the β-carotene is often used to reflect the reducing environment, indicating the salinity and stratification of lake water. Its abundance is usually expressed as β-carotane/*n*-C_{max}. Moreover, the content of the β-carotane in marine and continental oil shale varies greatly. The content of β-carotane is very low in marine oil shale and almost lacks this compound. While in continental oil

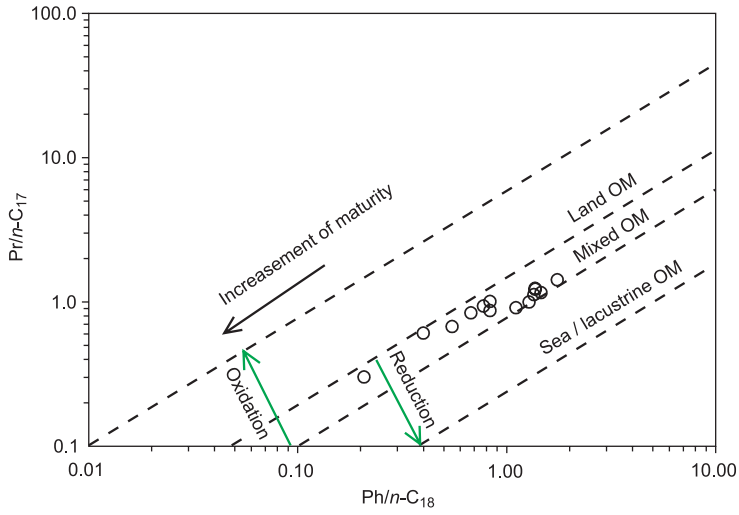

Fig. 4. Crossplot of Pr/*n*-C_{17} and Ph/*n*-C_{18} (modified from (Shanmugam, 1985)).

shale, the β-carotane has a certain content. Therefore, in continental shale formations, the β-carotane is a good parameter for judging paleo-oxygen. The β-carotane was detected in 10 out of 14 samples. The quality scores ranged from 0.38 to 24.94, with an average of 4.84 (Fig. 3), indicating a high degree of the β-carotane. The distribution of *w*(β-carotane)/*w*(*n*-C_{max}) is between 0.05 and 3.72, with an average value of 0.71. Only one of the 10 detected samples has a *w*(β-carotane)/*w*(*n*-C_{max}) value greater than 2 (Fig. 3), indicating a semi-oxidation and semi-reduction salinization environment.

In addition, the Pr/*n*-C_{17} and Ph/*n*-C_{18} values of acyclic isoprene alkanes are also used to explain the parent material type and depositional environment of source rocks. The correlation between Pr/*n*-C_{17} and Ph/*n*-C_{18} can also be used to determine the maturity of hydrocarbon source rocks and the degree of biodegradation (Connan and Cassou, 1980). According to the relationship diagram of Pr/*n*-C_{17} and Ph/*n*-C_{18} of the samples, it is believed that the parent material of the Second member of the Lucaogou Formation formed in a semi-oxidative and semi-reducing environment, which verifies the β-carotane judgment result (Fig. 4).

Paleosalinity

Gammacerane is a triterpenoid of C_{30}, and its predecessor is tetramethylene alcohol. Widely distributed in protozoa and photosynthetic sulfur bacteria, belonging to salt-loving protists. It is frequently found in high salinity saline terrestrial and marine sediments. Therefore, it is generally believed that the high content of gammacerane is a sign of the depositional environment of high-salinity water bodies. But not all high salinity environments can detect high levels of gammacerane. In some freshwater-brackish lacustrine deposits, there are high levels of gammacerane instead. Therefore, when using gammacerane to study water salinity, it should be supported by other evidence. In addition, the presence of gammacerane may be related to the salinity stratification of the sedimentary water (Moldowan et al., 1985; Peters and Moldowan, 1993; Damsté et al., 1995; Zhang et al., 1999).

Gammacerane is commonly detected in the samples. The value of the *w*(gammacerane)/*w*(C_{30} hopane) is between 0.09 and 0.30, with an average value of 0.17. The *w*(gammacerane)/*w*(C_{31}R hopane) ranges from 0.46 to 1.19, with a mean of 0.78. The *w*(gammacerane)/*w*(C_{31} homohopane) ranges from 0.58 to 1.47, with a mean of 1.04 (Table 2). The *w*(gammacerane)/*w*(C_{30} hopane) correlates well with *w*(gammacerane)/*w*(C_{31}R hopane) and *w*(gammacerane)/*w*(C_{31} homohopane). The R^2 values were 0.74 and 0.52, respectively. Previous studies have found that water stratification and low oxygen content at higher salinity will lead to lower Pr/Ph value. That is, there is a significant negative correlation between the Pr/Ph and the gammacerane index, and the high gamma waxane content only occurs at higher salinity (Peters et al., 2005; Hu et al., 2006). The Pr/Ph of the samples is mainly distributed between 0.80 and 1.33 (Table 2). The negative correlation between the Pr/Ph and the gammacerane index is poor. The R^2 is only 0.15. This shows that the salinity and reducibility of sedimentary water in the Second member of the Lucaogou Formation are not very high, and the water stratification is not obvious. This further supports the idea that the sedimentary paleoenvironment was characterized by a semi-oxidative and semi-reductive environment.

CHARACTERISTICS OF ORGANIC MATTER

Parent material types

The *n*-alkanes are derived from living organisms or lipid compounds such as fatty acids and waxes. Odd-carbon *n*-alkanes with high molecular weight (*n*-C_{25}~*n*-C_{33}) are mainly derived from the keratin waxes of higher plants and often appear in organic matter rich in higher plants and the crude oil they produce. Constant odd carbon number advantage can be expressed by CPI and OEP values (Mamaseni et al., 2019). Odd-carbon *n*-alkanes with medium molecular weight (*n*-C_{15}~*n*-C_{23}) often appear in hydrocarbon compounds generated from organic matter in marine or deep lacustrine sediments. Derived from algae and aquatic plankton, with

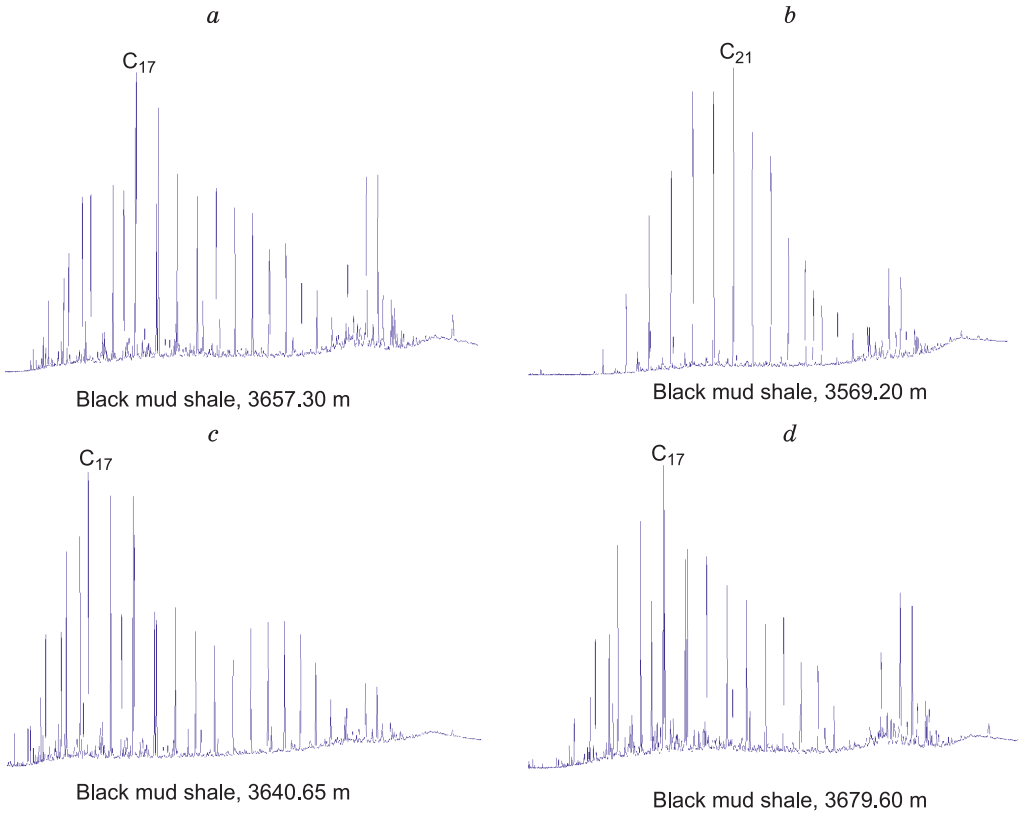

Fig. 5. Chromatogram of *n*-alkanes in the Second member of the Lucaogou Formation.

n-C_{15} and *n*-C_{17} as the main peaks, formed by decarboxylation of *n*-C_{16} and *n*-C_{18} fatty acids in phytoplankton or benthic algae. The *n*-alkanes with the predominance of even carbon numbers often appear in carbonate rocks or evaporite series, and are formed by the reduction of *n*-fatty acids, alcohols, phytane and phytanol in a reducing environment. Therefore, different parent material types will cause *n*-alkanes to have different compound composition characteristics, and these characteristics will form different carbon number distribution curve characteristics on the chromatogram. There are usually three basic types: pre-peak, post-peak and bimodal. The pre-peak type reacts the parent material types is dominated by lower aquatic organisms, the main peak carbon is mainly low carbon number alkanes, and the high carbon number is less; The parent material types of the post-peak is mainly terrigenous higher plants, the main peak carbon is mainly high carbon number alkanes, and there is an obvious odd carbon advantage. The bimodal type represents that the parent material types has the characteristics of mixed origin of lower aquatic organisms and higher plants at the same time. In addition, it has been shown that submerged, emerging/floating macrophytes are an important source of *n*-alkanes with medium molecular carbon numbers (*n*-C_{21}, *n*-C_{23}, *n*-C_{25}) (Cranwell, 1984; Viso et al., 1993). The parameter of *Paq*[(*n*-C_{23} + *n*-C_{25})/(*n*-C_{23}+*n*-C_{25}+*n*-C_{29}+*n*-C_{31})] can reflect the contribution of large aquatic plants such as submerged plants, floating plants and emergent plants (Ficken et al., 2000). A *Paq*<0.1 corresponds to terrestrial plants, a *Paq* in the range 0.1–0.4 corresponds to emergent plants, and a *Paq* between 0.4 and 1 corresponds to submerged plants. In addition, the *n*-C_{23}/*n*-C_{29} and *n*-C_{23}/*n*-C_{31} values reflect the relative abundance of peat moss relative to other higher plants. The lower values of *n*-C_{23}/*n*-C_{29} and *n*-C_{23}/*n*-C_{31} reflect the low relative abundance of peat moss (Nott et al., 2000; Nichols et al., 2006).

The spectrum of *n*-alkanes in the mud shale samples is mainly “bimodal”. The main peak carbon number is inconsistent, dominated by low and medium carbon numbers (Fig. 5). The values of $\Sigma C^{-}_{21}/\Sigma C^{+}_{22}$ ranged from 0.31 to 2.60, with an average value of 1.19 (Table 3). There are 10 samples greater than 1, accounting for 71.43% of all samples. It shows that lake-phase algae dominate the organic matter input, and terrestrial higher plants are mixed in a certain proportion. The value of *Paq* in the samples is between 0.67 and 1.00, with an average value of 0.85. It reflects the contribution of lake-submerged plants (algae) to the parent material. The C_{29} was detected in 10 of the 14 mud shale samples, and the *n*-C_{23}/*n*-C_{29} values ranged from 1.39 to 7.11, with an average value of 3.27. The C_{31} was detected in only 6 of the 14 samples. And the *n*-C_{23}/*n*-C_{31} ranged from 3.73 to 7.13, with an average value of 5.18 (Table 3). The values of the *n*-C_{23}/*n*-C_{29} and *n*-C_{23}/*n*-C_{31} indicate that the abundance of peat moss plants is low compared to other higher plants.

Table 3. **Saturated hydrocarbon chromatography, organic carbon pyrolysis and chloroform asphalt data**

Sample No.	$\Sigma C_{21}/\Sigma C_{22}^{+}$	n-C_{23}/n-C_{29}	n-C_{23}/n-C_{31}	OEP	CPI	IH, mg/g	TOC, %	S_1+S_2, mg/g	S_1, mg/g	S_2, mg/g	T_{max}, °C	"A", %
1	1.08	2.98	–	1.15	1.28	676.56	12.20	84.16	1.62	82.54	444	0.38
2	0.64	1.39	–	1.21	1.21	730.86	9.82	72.87	1.10	71.77	449	0.30
3	1.00	2.28	3.73	1.14	1.14	669.82	7.09	50.62	3.13	47.49	448	1.19
4	1.39	6.00	–	1.12	1.32	734.27	6.42	47.84	0.70	47.14	449	0.38
5	0.76	2.09	3.83	1.10	1.18	661.18	4.07	27.56	0.65	26.91	445	2.09
6	1.01	–	–	1.17	1.17	638.69	4.29	27.94	0.54	27.40	449	0.10
7	1.42	–	–	1.09	1.16	822.69	7.80	64.95	0.78	64.17	448	0.19
8	0.76	2.59	7.13	1.32	1.27	769.92	5.22	40.6	0.41	40.19	449	0.13
9	1.86	3.21	–	1.23	1.10	665.78	4.12	28.15	0.72	27.43	449	0.37
10	0.31	1.44	5.42	0.70	0.98	671.78	6.91	47.35	0.93	46.42	446	0.10
11	1.62	7.11	–	1.25	1.25	450.00	2.30	14.6	4.25	10.35	435	1.65
12	1.13	–	–	1.10	1.56	574.09	5.52	32.94	1.25	31.69	446	0.06
13	2.60	–	–	1.27	1.31	671.91	3.56	24.38	0.46	23.92	447	0.03
14	1.05	3.63	5.80	1.15	1.19	500.41	2.42	18.89	6.78	12.11	435	1.95

In addition, the values of Pr/n-C_{17} and Ph/n-C_{18} are commonly used to identify parent material types (Shanmugam, 1985). Figure 4 shows that the samples are located in regions of mixed OM, indicating that the Second member of the Lucaogou Formation is mixed source organic matter. The results obtained by this method are consistent with the discriminant results of the carbon number characteristics of n-alkanes. It shows the reliability of the conclusion. Meanwhile, Fig. 4 provides additional evidence that the depositional environment of the Second member of the Lucaogou Formation is a semi-oxidizing and semi-reducing environment.

Steranes in geosomes are evolved from biosynthetic sterols. Steroids are generally used for the discrimination of raw oil parent material type, identification of parent material deposition environment (Huang and Meinshein, 1979). The aquatic plankton is dominated by C_{27} sterane, and the content of C_{28} and C_{29} sterane is low; while the terrestrial organisms are dominated by C_{29} sterane, and the content of C_{27} and C_{28} sterane is low (Moldowan et al., 1985; Shanmugam, 1985). During the evolution of organic matter, C_{27}, C_{28} and C_{29} in bioorganic matter are dehydroxylated to steranes of the same carbon number, while their carbon skeletons remain unchanged. Therefore, the contribution ratio of different biological sources can be determined according to the relative content of C_{27}, C_{28} and C_{29} in crude oil or source rock extracts.

The contents of C_{27}, C_{28} and C_{29} in 10 of the 14 samples showed a sequential increasing trend. Only two samples had high C_{28} sterane content, and C_{27}, C_{28} and C_{29} showed an inverted "V" shape. It reflects that the input of terrestrial organisms is obvious. In addition, from the C_{27}–C_{28}–C_{29} triangular distribution map of bioconfiguration steranes [AAA(R)], it can be found that the organic matter of the samples mainly originated from the mixed input of higher plants and algae together (Fig. 6).

Combining the above discriminatory results, the parent material of the mud shale samples from the Second member of the Lucaogou Formation is considered to be a mixture of terrestrial higher plants and lacustrine lower organisms. The input proportion of lacustrine is slightly higher that thanterrestrial higher plants.

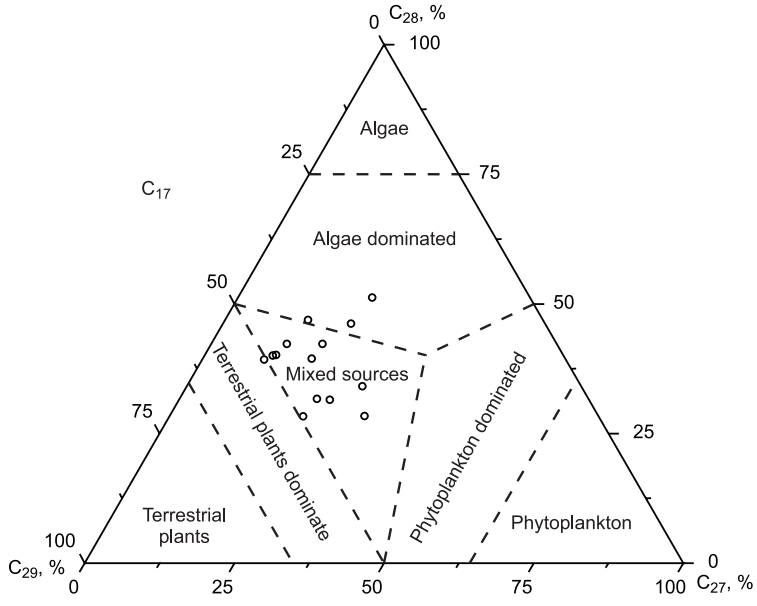

Fig. 6. The AAA(R) configuration of the C_{27}–C_{28}–C_{29} sterane triangle diagram.

ORGANIC MATTER MATURITY

The rock pyrolysis analysis showed that the T_{max} values of the samples were distributed between 435 and 457 °C, with an average value of 446 °C (Table 3), indicating that the organic matter is in the mature stage (oil window). With the increase of thermal evolution degree, the unstable biological configuration of steranes and terpenoids gradually changes to a stable configuration. Therefore, they are often used to characterize the degree of the thermal evolution of organic matter.

Hophanes are generally derived from polyhydroxy hopanes in prokaryotes, and their precursors exist in bacteria and blue-green algae, and some tropical trees and lower plants also contain their precursors (Killops and Howell, 1991; Moldowan et al., 1991; Telnaes et al., 1992; Nytoft et al., 2006). During the evolution of organic matter, hopanes undergo specific isomerization transitions. With the increase of thermal evolution degree, the 17β(H), 21β(H) biotype will change to 17β(H), 21α(H) and then 17α(H), 21β(H) geotype. At the same time, the 22R configuration will be converted to the 22S configuration (Dai et al., 2000). Therefore, the 22S/(22S+22R) of the C_{31} hopane can be used as an indicator for judging the maturity of the organic matter. According to the results of the mass chromatogram (MRM/GC-MS, m/z = 191), the terpenoids of the samples were mainly pentacyclic triterpene alkane series compounds, the content of tricyclic terpenes and tetracyclic terpenes was relatively low, and the peak height and peak area in the spectrum were small and low resolution. The 22S/(22S+22R) value of C_{31} hopane ranges from 0.54 to 0.61, with an average value of 0.57 (Table 2), which reflects the high maturity of the samples in the study area. In addition, the isomerization parameters of C_{27} rearranged steranes are suitable for the mature or high maturity stage (Peters et al., 2005; Lu, 2008). The value of the $w(C_{27}$ rearranged sterane 20S)/[$w(C_{27}$ rearranged sterane 20(S+R)] is 0.13–0.72, with an average value of 0.44 (Table 2), which is close to the isomerization equilibrium value of 0.6. This indicates that the source rock has at least entered the oil generation threshold (equivalent to a R_o value of about 0.6%) (Peters and Moldowan, 1993; Ren et al., 2000).

In the process of evolution of steroids, the carbon atom will undergo a process of transformation from R biological configuration to S geological configuration, so that the regular sterane 14,17(H) undergoes a transformation from αα to ββ position (Dai et al., 2000). Therefore, the C_{29}20S/(20S+20R) and C_{29}ββ/(ββ+αα) of C_{29} sterane can also be used as indicators of organic matter maturity (Huang et al., 1990; Peters et al., 2005). The αααC_{29}20S/(20S+20R) and C_{29}ββ/(ββ+αα) of sterane isomerization are good biomarker compound parameters indicative of organic matter maturity (Moldowan et al., 1991). As the maturity increases, their values gradually increase, reaching equilibrium values of 0.5 (Seifert and Moldowan, 1986) and 0.7 (Peters and Moldowan, 1993) for the maturity stage, respectively. The C_{29}20S/(20S+20R) and C_{29}ββ/(ββ+αα) values in the extracts from the samples range from 0.38 to 0.54 and 0.29 to 0.40, respectively (Table 2). It is commonly accepted that the C_{29}20S/(20S+20R) value reaching 0.2 represents the limit of the oil-generating window of shale. A value less than 0.2 indicates an immature stage, while a value of 0.55 is the equilibrium value at the end of thermal evolution. Based on the C_{29}20S/(20S+20R) and C_{29}ββ/(ββ+αα) rendezvous plots of the samples, it is found that the mud shale of the Second member of the Lucaogou Formation has reached maturity above (Fig. 7).

The odd-even predominance index (OEP) is a parameter for judging the maturity of organic matter by the odd-even carbon predominance of *n*-alkanes. It is generally believed that the OEP value is 1.0–1.2 for mature

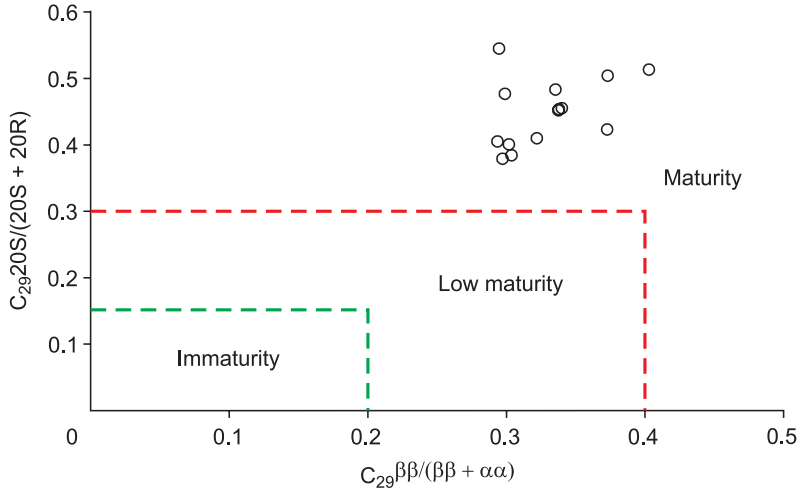

Fig. 7. Cross plot of the C_{29}S/(20S+20R) and C_{29}ββ/(ββ+αα).

organic matter, 1.2–1.4 for low-mature organic matter, and >1.4 for immature organic matter. The higher the OEP value, the lower the organic matter maturity. The closer the OEP value is to 1.0, the higher the organic matter maturity (Scalan and Smith, 1970). The OEP value of the samples ranges from 0.70 to 1.32, with an average value of 1.14. Samples with OEP values between 1.0 and 1.2 accounted for 57.14% of the total, samples with OEP values between 1.2 and 1.4 accounted for 35.71% (Table 3). It shows that the source rocks of the Second member of the Lucaogou Formation are mainly in the mature stage. Similarly, there is the carbon dominance index (CPI), a parameter that reflects the relative abundance between odd-numbered carbon atoms and even-numbered carbon atoms of the *n*-alkanes. The CPI values in modern sediments range from 2.4 to 5.5; in crude oil, the CPI value is 1; in ancient sedimentary rocks, with their organic matter maturity, the CPI values range is 2.4–1 (Bray and Evans, 1961). The CPI values of the samples range from 0.98 to 1.56, with a mean value of 1.22. Only one of the 14 samples had a CPI value of less than 1, while the remaining 13 samples had a CPI value greater than 1 (Table 3). It means that the maturity of the samples all reach above the raw oil threshold. In addition, the Ts/(Ts+Tm) values are generally used to assist in determining the maturity of organic matter (Seifert and Moldowan, 1978). The value of Ts/(Ts + Tm) usually increases with the maturity increasement. At a R_o value of about 1.4%, the value of Ts /(Ts + Tm) can reach the equilibrium value of 1 (Peters and Maldowan, 1993; Zhao et al., 2016). The Ts/(Ts+Tm) values of the extracts from the samples ranges from 0.04 to 0.32, with an average of 0.11 (Table 2), indicating a high maturity.

It is important to note that high maturity may have the effects on biomarker compounds. Dzou et al. (1995) suggested that when organic matter is at higher levels of maturity, these molecular source indicators take on a more "marine" or "deep-water lacustrine" signature. They gave the limits of this influence: $R_o > 1.1\%$; one component is initially present in much higher concentration than the other (e.g., C_{29} sterane >> C_{27} sterane; pristane >> phytane) (Dzou et al., 1995). Figure 8 shows that the increase in T_{max} does not result in a significant decrease in Pr/Ph and C_{29}/C_{27} sterane. Samples with T_{max} close to 450 °C also did not exhibit such characteristics: C_{29} spine>>C_{27} spine; pristane >> phytane (Fig. 8). Therefore, we consider the results of paleo-sedimentary and parent marerial types obtained using the source-dependent molecular paremeters is reliable.

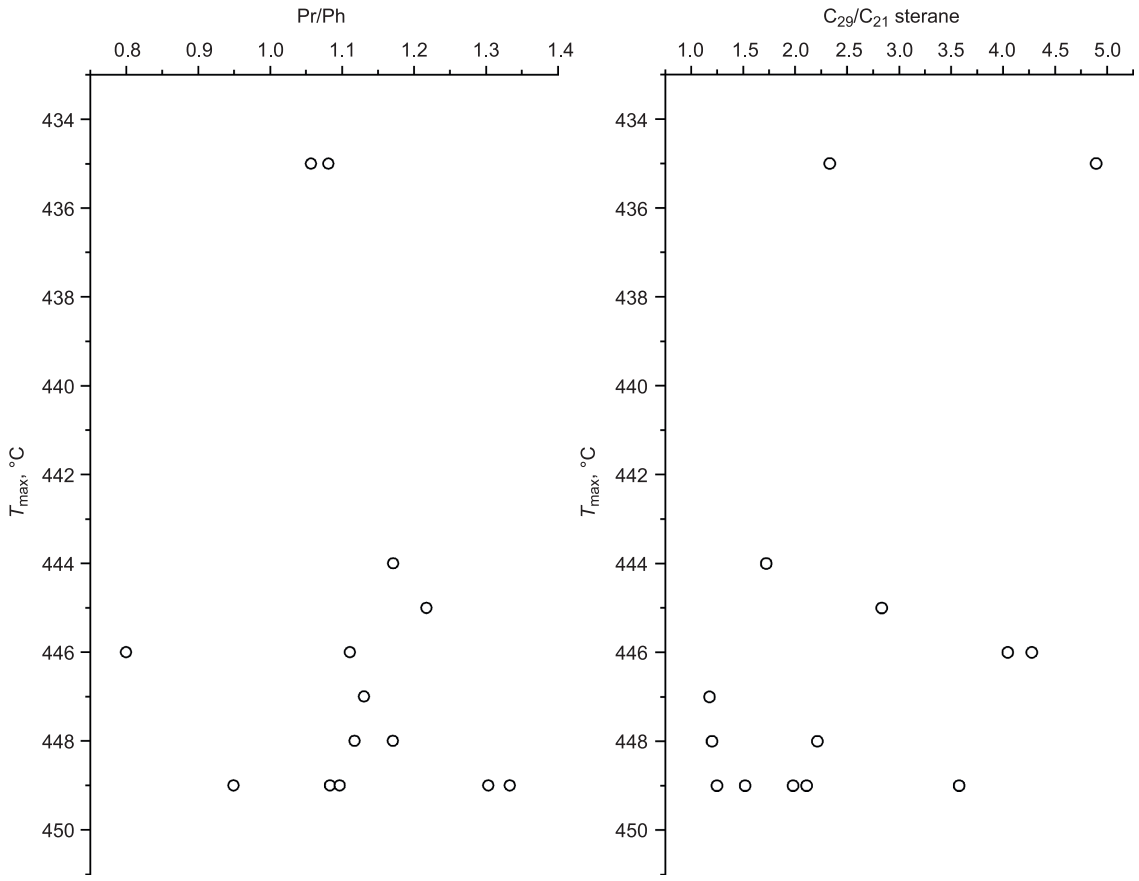

Fig. 8. Plots showing the variations of Pr/Ph ratio and C_{29}/C_{27} sterane with maturity (T_{max}).

OIL-BEARING PROPERTY AND SHALE OIL SIGNIFICANCE

The TOC values of the second section mud shale of the Lucaogou Formation range from 2.30 to 12.20%, with an average value of 5.84%. The content of chloroform bitumen ("A") is 0.03–2.09%, with an average of 0.64% (Fig. 9). Hydrocarbon generation potential (S_1+S_2) is mainly distributed between 14.60 and 84.18 mg/g, with an average of 41.63 mg/g. The range of S_1 value is 0.41–6.78 mg/g, with an average of 1.67 mg/g; the S_2 value ranges from 10.35 to 82.54 mg/g, with an average of 39.97 mg/g (Table 3). Based on the Evaluation criteria for organic matter of terrestrial hydrocarbon source rock (SY/T5735, 1995), the second section mud shale of the Lucaogou Formation generally reached the good–best oil-bearing rock standard.

The distribution of hydrogen index (IH) ranges from 450 to 822.69 mg/g, with an average value of 659.85 mg/g (Table 3). The diagram of I_H vs. T_{max} (Espitalie et al., 1985) showed that the organic matter type of the samples was predominantly type I, and only two samples were type II (Fig. 10).The problem is that the hydrogen index increases with the total organic carbon content. Therefore the diagram of I_H vs. T_{max} may exaggerate the type I organic matter type of the samples. The diagram of S_2 vs. TOC can avoid the problem of increasing hydrogen index with total organic carbon content (Langford and Blanc-Valleron, 1990). The dividing line for I–II is HI = 700 mg/g and for II-III is HI = 200 mg/g. The organic matter types of the samples were type I and II (Fig. 10). It should be noted that, the slope of the I–II boundary decreases with increasing maturity. About half of the samples have a T_{max} close to 450 °C, which is high maturity. The slope of the I–II limit may be less than 700, so the percentage of type I organic matter may be a bit more.

Usually the components of rock extracts mainly include saturated hydrocarbons, aromatic hydrocarbons, non-hydrocarbons and asphaltenes, and the different ratios can reflect the physical properties of organic hydrocarbons. The content of saturated hydrocarbon fractions in the samples ranged from 15.07 to 52.49%, with an average of 34.10%. The content of aromatic hydrocarbons is 8.05–20.88%, the average is 15.39%. The ratio of saturated hydrocarbons to aromatic hydrocarbons fluctuates greatly, ranging from 0.77 to 6.52, with an average of 2.54. The asphaltene content ranges from 1.94 to 19.17%, with an average of 10.14%. The colloid content ranges from 20.37 to 54.25%, with an average of 37.13% (Table 1). This results in a medium to upper-medium density of shale oil in the Lucaogou Formation, ranging from 0.87 to 0.90 (Table 1). The saturated hydrocarbon carbon numbers of the samples ranged from n-C_{13} to n-C_{33}, and the spectral distribution pattern showed a bimodal shape (Fig. 5). The main peak carbon is mainly n-C_{17} and n-C_{23}, dominated by medium-low molecular weight alkanes. At the same time, $\Sigma C_{21}/\Sigma C_{22}^{+}$ represents the ratio of light components/heavy components, re-

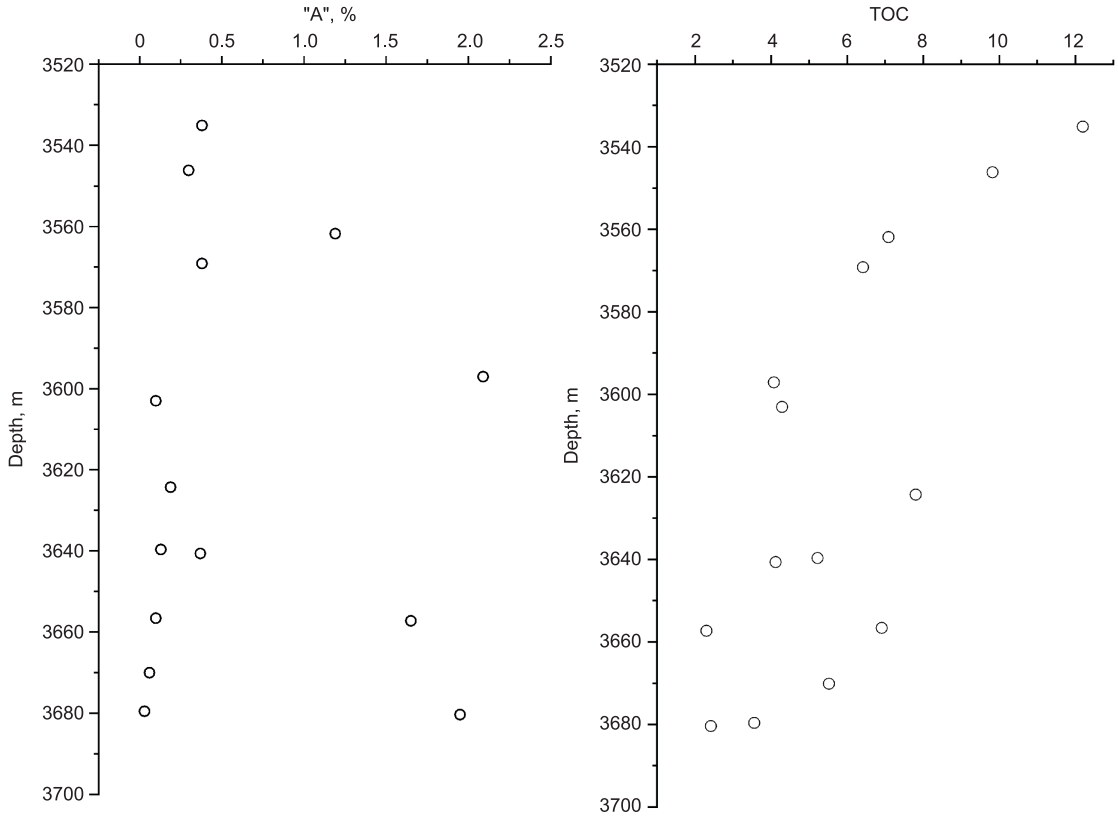

Fig. 9. Plots showing the variations of "A", % and TOC with depth, m.

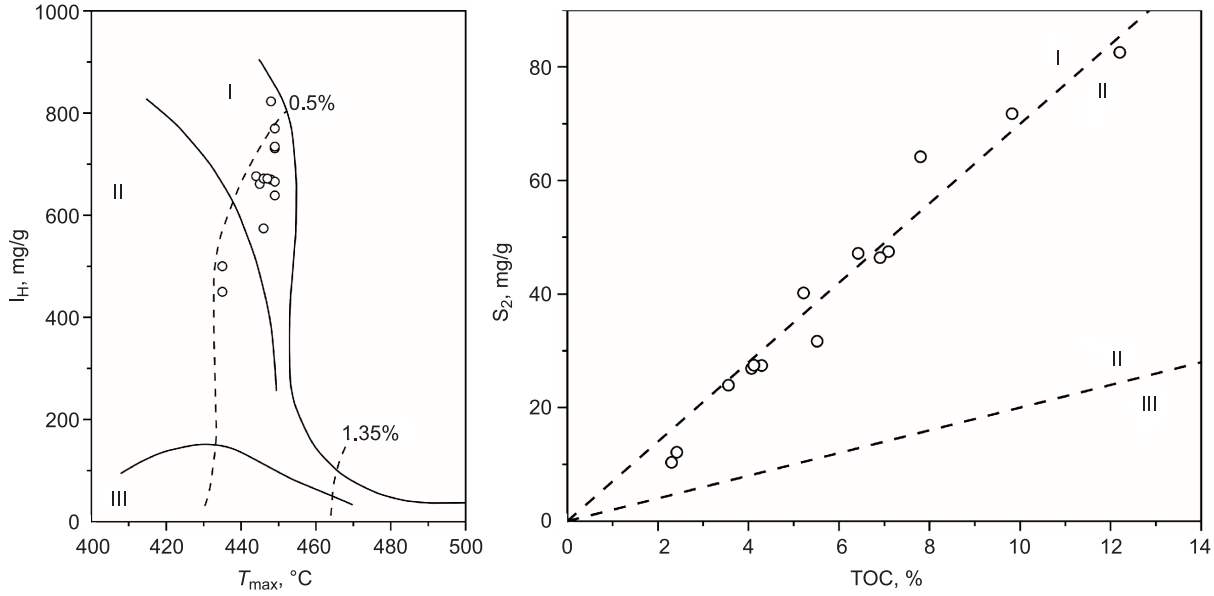

Fig. 10. Organic matter type classification diagram by rock-eval parameters.

flecting the change of the carbon number of the main peak of saturated hydrocarbons. A ratio greater than 1 reflects the short-chain advantage, while a ratio less than 1 reflects the long-chain advantage. The $\Sigma C^{-}_{21}/\Sigma C^{+}_{22}$ values of the samples are distributed between 0.31 and 2.60, with an average value of 1.19 (Table 3). The samples greater than 1 accounted for 71.43% of all samples. It shows that the saturated hydrocarbons in the mud shale samples are mainly light components with short chains.

The Lucaogou Formation contains abundant shale oil resources. Substantial breakthroughs have been made in the Second member of the Lucaogou Formation in rencent years. The thickness of the mud shale reservoir ranges from 10 to 25 m, with a maximum cumulative thickness of 25 m and a distribution area of about 600 km^2. At the same time, the mud shale of the Second member of Lucaogou Formation in Jimsar sag has a high content of chloroform bitumen "A", high content of saturated hydrocarbon components, and low asphaltene content. The main peak carbons of *n*-alkanes are *n*-C_{17} and *n*-C_{23} which tend to medium-low molecular weight alkanes. The light component/heavy component value reflects the short-chain advantage. Therefore, the mud shale of the Second member of the Lucaogou Formation in Jimsar sag has the huge exploration potential of shale oil. Based on the breakthrough in the exploration and development of the "sweet spots", i.e., silt-fine sandstones, carbonatites (Si et al., 2013; Cao et al., 2016; Wang et al., 2020), the next step should be to focus on the exploration of shale oil in the pure mud shale layer. It is essential to conduct forward-looking and exploratory research on pure mud shale layer, which will provide a geological basis and key parameters for the exploration and development of pure mud shale oil in the Second member of the Lucaogou Formation in the Jimsar sag.

CONCLUSIONS

The sedimentary environment of the mud shale of the Second member of the Lucaogou Formation in the Jimsar sag is semi-oxidative and semi-reductive. The parent material is mainly aquatic with minor input of higher plants. Organic matter type is type I–II. Hydrocarbon source rocks have a high degree of maturity.

The distribution of TOC values of the Second member of the Lucaogou Formation ranges from 2.30 to 12.2%, with an average of 5.84%. The content of mud shale chloroform bitumen "A" is 0.03–2.09%, the average is 0.64%. The hydrocarbon generation potential (S_1+S_2) was mainly distributed between 14.60 and 84.16 mg/g with an average of 41.63 mg/g. The value of the pyrolysis parameter (T_{max}) ranges from 435 to 449 °C, with an average value of 446 °C. Belong to high quality hydrocarbon source rock with good oil-bearing property.

The mud shale extracts from the Second member of the Lucaogou Formation have high content of saturated hydrocarbon fraction (34.10% on average), large average saturation/aromatic value (2.54 on average) and low asphaltene content (10.14% on average). The average value of the $\Sigma C^{-}_{21}/\ \Sigma C^{+}_{22}$ is 1.19, which is greater than 1.00, reflecting the advantage of alkanes with short chains. The main peak carbon is dominated by *n*–C_{17} and *n*–C_{23}, with a preference for medium to low molecular weight alkanes. It indicates that there is great potential for shale oil exploration in the pure mud shale of the Second member of the Lucaogou Formation in the Jimsar sag.

We are grateful to the financial support from the Research Institute of Experiment and Detection, Petro China Xinjiang Oilfield Company. We truly appreciate the assistance of Professor Aimin Jin and Yifeng Liu for

their guidance in the writing process of the article. We also would like to acknowledge our indebtedness to the editor and reviewers for their kind work and comments.

REFERENCES

Bai, H., Pang, X.Q., Kuang, L.C., Pang, H., Wang, X.L., Jia, X.Y., Zhou, L.M., Hu, T., 2017. Hydrocarbon expulsion potential of source rocks and its influence on the distribution of lacustrine tight oil reservoir, Middle Permian Lucaogou Formation, Jimsar Sag, Junggar Basin, Northwest China. J. Pet. Sci. Eng. 149, 740–755, doi: 10.1016/j.petrol.2016.09.053.

Bray, E.E., Evans, E.D., 1961. Distribution of *n*-paraffins as a clue to recognition of source beds. Geochim. Cosmochim. Acta 22, 2–15, doi: 10.1016/0016-7037(61)90069-2.

Cao, Z., Liu, G., Kong, Y., Wang, C., Niu, Z., Zhang, J., Geng, C., Shan, X., Wei, Z., 2016. Lacustrine tight oil accumulation characteristics: Permian Lucaogou Formation in Jimusaer Sag, Junggar Basin. Int. J. Coal Geol. 153, 37–51, doi: 10.1016/j.coal.2015.11.004.

Cao, Z., Liu, G., Xiang, B., Wang, P., Wang, C., 2017. Geochemical characteristics of crude oil from a tight oil reservoir in the Lucaogou Formation, Jimusar sag, Junggar basin. AAPG Bull., 101, 39–72, doi: 10.1306/05241614182.

Connan, J., Cassou, A.M., 1980. Properties of gases and petroleum liquids derived from terrestrial kerogen at various maturation levels. Geochim. Cosmochim. Acta 44, 1–23, doi: 10.1016/0016-7037(80)90173-8.

Cranwell, P.A., 1984. Lipid geochemistry of sediments from Upton Broad, a small productive lake. Org. Geochem. 7, 25–37, doi: 10.1016/0146-6380(84)90134-7.

Dai, H.M., Wang, S.Y., Chen, Y.C., 2000. Geochemistry of Oil and Gas Exploration. Petroleum Industry Press, Beijing, pp. 160–161.

Damsté, J.S.S., Kenig, F., Koopmans, M.P., Köster, J., Schouten, S., Hayes, J.M., de Leeuw, J.W., 1995. Evidence for gammacerane as an indicator of water column stratification. Geochim. Cosmochim. Acta. 59, 1895–1900, doi: 10.1016/0016-7037(95)00073-9.

Didyk, B.M., Simoneit, B., Brassell, S.C., Eglinton, G., 1978. Organic geochemical indicators of palaeoenvironmental conditions of sedimentation. Nature 272, 216–222, doi: 10.1038/272216a0.

Du, J.H., Hu, S.Y., Pang, Z.L., Lin, S.H., Hou, L.H., Zhu, R.K., 2019. The types, potentials and prospects of continental shale oil in China. China Pet. Explor. 24, 560–568.

Dzou, L., Noble, R.A., Senftle, J.T., 1995. Maturation effects on absolute biomarker concentration in a suite of coals and associated vitrinite concentrates. Org. Geochem. 23, 681–697, doi: 10.1016/0146-6380(95)00035-D.

Eidsnes, H., 2014. Structural and stratigraphic factors influencing hydrocarbon accumulations in the Bakken Petroleum System in the Elm Coulee field, Williston Basin, Montana. PhD Thesis. Colorado School of Mines.

Espitalie, J., Deroo, G., Marquis, F., 1985. Rock-Eval pyrolysis and its applications (part 2). Oil Gas Sci. Technol. 40, 755–784, doi: 10.2516/ogst:1985045.

Evaluation Criteria for Organic Matter of Terrestrial Hydrocarbon Source Rock: SY/T 5735, 1995. Petroleum Industry Press, Beijing.

Fang, S., Jia, C., Guo, Z., Song, Y., Xu, H., Liu, L., 2006. New view on the Permian evolution of the Junggar Basin and its implications for tectonic evolution. Earth Sci. Front. 13 (3), 108–121.

Ficken, K.J., Li, B., Swain, D.L., Eglinton, G., 2000. An *n*-alkane proxy for the sedimentary input of submerged/floating freshwater aquatic macrophytes. Org. Geochem. 31, 745–749, doi: 10.1016/S0146-6380(00)00081-4.

Gao, Y., Ye, Y.P., He, J.X., Qian, G.B., Qin, J.H., Li, Y.Y., 2020. Development practice of continental shale oil in the Jimsar sag in the Junggar Basin. China Pet. Explor. 25, 133–141, doi: 10.3969/j.issn.1672-7703.2020.02.013.

Hou, L.H., Yu, Z.C., Luo, X., Lin, S.H., Zhao, Z.Y., Yang, Z., Wu, S.T., Cui, J.W., Zhang, L.J., 2021. Key geological factors controlling the estimated ultimate recovery of shale oil and gas: A case study of the Eagle Ford shale, Gulf Coast Basin, USA. Pet. Explor. Dev. 48, 762–774, doi: 10.1016/S1876-3804(21)60062-9.

Hu, Y., Zhang, Z.H., Li, W., Wu, S.P., 2006. Molecular biomarkers characteristics of source rocks from Tanhai Sanma area in the Huanghua Depression and its signification for sedimentary facies. Acta Sediment. Sinica 24 (3), 419–425.

Hu, S.Y., Zhao, W.Z., Hou, L.H., Yang, Z., Zhu, R.K., Wu, S.T., Bai, B., J.X., 2020. Development potential and technical strategy of continental shale oil in China. Pet. Explor. Dev. 47, 877–887, doi: 10.1016/S1876-3804(20)60103-3.

Hu, S.Y., Bai, B., Tao, S., Bian, C., Zhang, T., Chen, Y., Liang, X., Wang, L., Zhu, R., Jia, J., 2022. Heterogeneous geological conditions and differential enrichment of medium and high maturity continental shale oil in China. Pet. Explor. Dev. 49, 257–271, doi: 10.1016/S1876-3804(22)60022-3.

Huang, W.Y., Meinshein, W.C., 1979. Sterols as ecological indicators. Maturation sequence of continental crude oils in hydrocarbon basins in China and its significance. Geochim. Cosmochim. Acta 43, 739–745, doi: 10.1016/0016-7037(79)90257-6.

Huang, D.F., Li, J.C., Zhang, D.J., 1990. Maturation sequence of continental crude oils in hydrocarbon basins in China and its significance. Org. Geochem. 16, 521–529, doi: 10.1016/0146-6380(90)90067-A.

Killops, S.D., Howell, V.J., 1991. Complex series of pentacyclic triterpanes in a lacustrine sourced oil from Korea Bay Basin. Chem. Geol. 91, 65–79, doi: 10.1016/0009-2541(91)90016-K.

Kong, X., Zeng, J., Tan, X., Ding, K., Wang, M., 2021. Natural tectonic fractures and their formation stages in tight reservoirs of Permian Lucaogou Formation, Jimsar Sag, southern Junggar Basin, NW China. Mar. Pet. Geol. 133, 105269, doi: 10.1016/j.marpetgeo.2021.105269.

Langford, F.F., Blanc-Valleron, M.M., 1990 Interpreting rock-eval pyrolysis data using graphs of pyrolizable hydrocarbons vs. total organic carbon. AAPG Bull. 74, 799–804, doi: 10.1306/0C9B238F-1710-11D7-8645000102C1865D.

Li, M.W., Ma, X.X., Jiang, Q.G., Li, Z.M., Pang, X.Q., Zhang, C.T., 2019. Enlightenment from formation conditions and enrichment characteristics of marine shale oil in North America. Pet. Geol. Recovery Effic. 26, 13–28, doi: 10.13673/j.cnki.cn37-1359/te.2019.01.002.

Li, Q., Liu, Z., Chen, F., Liu, G., Zhang, D., Li, P., Wang, P., 2022. Geochemical characteristics and organic matter provenance of shale in the Jurassic Da'anzhai Member, Northeastern Sichuan Basin. Front. Earth Sci. 10, 860477, doi: 10.3389/feart.2022.860477.

Lu, F., 2008. Petroleum Geochemical. Petroleum Industry Press, Beijing, pp. 200–212.

Mamaseni, W.J., Naqshabandi, S.F., Al-Jaboury, F.K., 2019. Hydrocarbon generation potential of Chia Gara Formation in three selected wells, northern Iraq. Open Geosci. 11, 77–88, doi: 10.1515/geo-2019-0007.

Moldowan, J.M., Fago, F.J., Carlson, R.M., Young, D.C., Duvne, G., Clardy, J., Schoell, M., Pillinger, C.T., Watt, D.S., 1991. Rearranged hopanes in sediments and petroleum. Geochim. Cosmochim. Acta 55, 3333–3353, doi: 10.1016/0016-7037(91)90492-N.

Moldowan, J.M., Seifert, W.K., Gallegos, E.J., 1985. Relationship between petroleum composition and depositional environment of petroleum source rocks. AAPG Bull. 69, 1255–1268, doi: 10.1306/AD462BC8-16F7-11D7-8645000102C1865D.

Nichols, J.E., Booth, R.K., Jackson, S.T., Pendall, E.G., Huang Y., 2006. Paleohydrologic reconstruction based on n-alkane distributions in ombrotrophic peat. Org. Geochem. 37, 1505–1513, doi: 10.1016/j.orggeochem.2006.06.020.

Nott, C.J., Xie, S., Avsejs, L.A., Maddy, D., Chambers, F.M., Evershed, R.P., 2000. *n*-Alkane distributions in ombrotrophic mires as indicators of vegetation change related to climatic variation. Org. Geochem. 31, 231–235, doi: 10.1016/S0146-6380(99)00153-9.

Nytoft, H.P., Lutnæs, B.F., Johansen, J.E., 2006. 28-*Nor*-spergulanes, a novel series of rearranged hopanes. Org. Geochem. 37, 772–786, doi: 10.1016/j.orggeochem.2006.03.005.

Pang, H., Pang, X.Q., Dong, L., Zhao, X., 2017. Factors impacting on oil retention in lacustrine shale: Permian Lucaogou Formation in Jimusaer Depression, Junggar Basin. J. Pet. Sci. Eng. 163, 79–90, doi: 10.1016/j.petrol.2017.12.080.

Peters, K.E., Moldowan, J.M., 1993. The Biomarker Guide: Interpreting Molecular Fossils in Petroleum and Ancient Sediments. 2nd ed. Cambridge University Press, Cambridge.

Peters, K.E., Walters, C.C., Moldowan, J.M., 2005. The Biomarker Guide. Cambridge University Press, Cambridge.

Peters, K.E., Walters, C.C., Moldowan, J.M., 2007. The Biomarker Guide. Vol. 2. Biomarkers and Isotopes in Petroleum Systems and Earth History. Cambridge University Press, Cambridge.

Powell, T.G., Mckirdy, D.M., 1973. Relationship between ratio of pristane to phytane, crude oil composition and geological environment in Australia. Nature 243, 37–39, doi: 10.1038/physci243037a0.

Qiu, Z., Tao, H.F., Zou, C.N., Wang, H.Y., Ji, H.J., Zhou, S.X., 2016. Lithofacies and organic geochemistry of the middle Permian Lucaogou Formation in the Jimusar Sag of the Junggar Basin, NW China. J. Pet. Sci. Eng. 140, 97–107, doi: 10.1016/j.petrol.2016.01.014.

Qu, C.S., Qiu, L.W., Cao, Y.C., Yang, Y.Q., Yu, K.H., 2019. Sedimentary environment and the controlling factors of organic-rich rocks in the Lucaogou Formation of the Jimusar Sag, Junggar Basin, NW China. Pet. Sci. 16, 763–775, doi: 10.1007/s12182-019-0353-3.

Ren, Y.J., Ji, Y.L., Li, R.X., 2000. Geochemical characteristics and significance of steranes and terpanes in the carboniferous potential source rocks of the South Qilian basin. Exp. Pet. Geol. 22, 341–345, doi: 10.11781/sysydz200004330.

Scalan, E.S., Smith, J.E., 1970. An improved measure of the odd-even predominance in the normal alkanes of sediment extracts and petroleum. Geochim. Cosmochim. Acta 34, 611–620, doi: 10.1016/0016-7037(70)90019-0.

Schoell, M., Hwang, R.J., Carlson, R.M.K., Welton, J.E., 1994. Carbon isotopic composition of individual biomarkers in gilsonites (Utah). Org. Geochem. 21, 673–683, doi: 10.1016/0146-6380(94)90012-4.

Seifert, W.K., Moldowan, J.M., 1978. Applications of steranes, terpanes and monoaromatics to the maturation, migration and source of crude oils. Geochim. Cosmochim. Acta 42, 77–95, doi: 10.1016/0016-7037(78)90219-3.

Seifert, W.K., Moldowan, J.M., 1986. Use of biological markers in petroleum exploration. Methods Geochem. Geophys. 24, 261–290.

Shanmugan, G., 1985. Significance of coniferous rain forests and related organic matter in generating commercial quantities of oil, Gippsland, Australia. AAPG Bull. 69, 1241–1254, doi: 10.1306/AD462BC3-16F7-11D7-8645000102C1865D.

Si, C.S., Chen, N.G., Yu, C.F., Li, Y.W., Meng, X.C., 2013. Sedimentary characteristics of tight oil reservoir in Permian Lucaogou Formation, Jimsar sag. Pet. Geol. Exp. 35, 528–533, doi: 10.11781/sysydz201305528.

Skvortsov, M.B., Dakhnova, M.V., Mozhegova, S.V., Kirsanov, A.M., Komkov, I.K., Paizanskaya, I.L., 2017. Geochemical methods for prediction and assessment of shale oil resources (case study of the Bazhenov Formation). Russ. Geol. Geophys. 58 (3–4), 403–409, doi: 10.1016/j.rgg.2016.09.015.

Telnaes, N., Isaksen, G.H., Farrimond, P., 1992. Unusual triterpane distributions in lacustrine oils. Org. Geochem. 18, 785–789, doi: 10.1016/0146-6380(92)90047-2.

Ten Haven, H.L., De Leeuw, J.W., Rullkötter, J., Damsté, J.S., 1987. Restricted utility of the pristane/phytane ratio as a palaeoenvironmental indicator. Nature 330, 641–643, doi: 10.1038/330641a0.

Tong, X.G., Zhang, G.Y., Wang, Z.M., Wen, Z.X., Tian, Z.J., Wang, H.J., Ma, F., Wu, Y.P., 2018. Distribution and potential of global oil and gas resources. Pet. Exp. Dev. 45, 727–736.

Viso, A.C., Pesando, D., Bernard, P., Marty, J.C., 1993. Lipid components of the Mediterranean seagrass *Posidonia oceanica*. Phytochemistry 34, 381–387, doi: 10.1016/0031-9422(93)80012-H.

Wang, Y., Cao, J., Tao, K., Gao, X., Shi, C., 2020. Multivariate statistical analysis reveals the heterogeneity of lacustrine tight oil accumulation in the Middle Permian Jimusar Sag, Junggar Basin, NW China. Geofluids 5, 1–14, doi: 10.1155/2020/1860219.

Wang, R., He, W.J., Zhao, X.M., Liu, G.L., Zhou, Z.M., Zhao, Y., 2022. Geological section analysis of shale oil in Lucaogou Formation of Well-Ji-174, Junggar Basin. Pet. Reservoir Eval. Dev. 12, 192–203, doi: 10.13809/j.cnki.cn32-1825/te.2022.01.017.

Wang, X.L., Zhang, G.S., Tang, W., Wang, D.H., Wang, K., Liu, J.Y., Du, D., 2022. A review of commercial development of continental shale oil in China. Energy Geosci. 3, 282–289, doi: 10.1016/j.engeos.2022.03.006.

Wu, H., Hu, W., Cao, J., Wang, X., Wang, X., Liao, Z., 2016. A unique lacustrine mixed dolomitic-clastic sequence for tight oil reservoir within the middle Permian Lucaogou Formation of the Junggar Basin, NW China: reservoir characteristics and origin. Mar. Pet. Geol. 76, 115–132, doi: 10.1016/j.marpetgeo.2016.05.007.

Xiao, W., Han, C., Yuan, C., Sun, M., Lin, S., Chen, H., Li, Z., Li J., Sun, S., 2008. Middle Cambrian to Permian subduction-related accretionary orogenesis of Northern Xinjiang, NW China: Implications for the tectonic evolution of central Asia. J. Asian Earth Sci. 32, 102–117, doi: 10.1016/j.jseaes.2007.10.008.

Yang, H., Niu, X.B., Xu, L.M., Feng, S.B., You, Y., Liang, X.W., Wang, F., Zhang D.D., 2016. Exploration potential of shale oil in Chang7 member, upper Triassic Yanchang Formation, Ordos Basin, NW China. Pet. Exp. Dev. 43, 560–569, doi: 10.1016/S1876-3804(16)30066-0.

Yang, Z., Zou, C.N., Wu, S.T., Lin, S.H., Jia, X.Y., 2019. Formation, distribution and resource potential of the "sweet areas (sections)" of continental shale oil in China. Mar. Pet. Geol. 102, 48–60, doi: 10.1016/j.marpetgeo.2018.11.049.

Zanin, Y.N., Eder, V.G., Zamirailova, A.G., 2008. Composition and formation environments of the Upper Jurassic–Lower Cretaceous black shale Bazhenov Formation (the central part of the West Siberian Basin). Mar. Pet. Geol. 25, 289–306, doi: 10.1016/j.marpetgeo.2007.07.009.

Zhang, L.P., Huang, D.F., Liao, Z.Q., 1999. Gammacerane-geochemical indicator of water column stratification. Acta Sediment. Sinica. 17, 136–140.

Zhao, W., Guo, X.W., He, S., 2016. Analysis on validity of maturity parameters of biomarkers: A case study from source rocks in Yitong basin. J. Xi'an Shiyou Univ. (Nat. Sci.). 31, 23–31, doi: 10.3969/j.issn.1673-064X.2016.06.004.

Zhao, W.Z., Hu, S.Y., Hou, L.H., Yang, T., Li, X., Guo, B.C., Yang, Z., 2020. Types and resource potential of continental shale oil in China and its boundary with tight oil. Pet. Exp. Dev. 47, 1–11, doi: 10.1016/S1876-3804(20)60001-5.

Zou, C.N., Zhi, Y., Cui, J.W., Zhu, R.K., Hou, L.H., Tao, S.Z., Yuan, X.J., Wu, S.T., Lin, S.H., Wang, L., Bai, B., Yao, J.L., 2013. Formation mechanism, geological characteristics and development strategy of nonmarine shale oil in China. Pet. Exp. Dev. 40, 15–27, doi: 10.1016/S1876-3804(13)60002-6.